frontiers in Molecular Biosciences

ORIGINAL RESEARCH
published: 08 November 2018
doi: 10.3389/fmolb.2018.00092

Millisecond Timescale Motions Connect Amino Acid Interaction Networks in Alpha Tryptophan Synthase

*Kathleen F. O'Rourke, Jennifer M. Axe, Rebecca N. D'Amico, Debashish Sahu and David D. Boehr**

Department of Chemistry, The Pennsylvania State University, University Park, PA, United States

Tryptophan synthase is a model system for understanding allosteric regulation within enzyme complexes. Amino acid interaction networks were previously delineated in the isolated alpha subunit (αTS) in the absence of the beta subunit (βTS). The amino acid interaction networks were different between the ligand-free enzyme and the enzyme actively catalyzing turnover. Previous X-ray crystallography studies indicated only minor localized changes when ligands bind αTS, and so, structural changes alone could not explain the changes to the amino acid interaction networks. We hypothesized that the network changes could instead be related to changes in conformational dynamics. As such, we conducted nuclear magnetic resonance relaxation studies on different substrate- and products-bound complexes of αTS. Specifically, we collected ^{15}N R_2 relaxation dispersion data that reports on microsecond-to-millisecond timescale motion of backbone amide groups. These experiments indicated that there are conformational exchange events throughout αTS. Substrate and product binding change specific motional pathways throughout the enzyme, and these pathways connect the previously identified network residues. These pathways reach the αTS/βTS binding interface, suggesting that the identified dynamic networks may also be important for communication with the βTS subunit.

Keywords: allostery, amino acid networks, enzyme dynamics, enzyme regulation, protein NMR, relaxation dispersion, tryptophan synthase

OPEN ACCESS

Edited by:
Andrea Mozzarelli, Università degli Studi di Parma, Italy

Reviewed by:
Barbara Cellini, University of Perugia, Italy
Patrick Senet, Université de Bourgogne, France
Leonard J. Mueller, University of California, Riverside, United States

***Correspondence:**
David D. Boehr
ddb12@psu.edu

Specialty section:
This article was submitted to Structural Biology, a section of the journal Frontiers in Molecular Biosciences

Received: *25 July 2018*
Accepted: *18 October 2018*
Published: *08 November 2018*

Citation:
O'Rourke KF, Axe JM, D'Amico RN, Sahu D and Boehr DD (2018) Millisecond Timescale Motions Connect Amino Acid Interaction Networks in Alpha Tryptophan Synthase. Front. Mol. Biosci. 5:92. doi: 10.3389/fmolb.2018.00092

INTRODUCTION

Allosteric regulation is a common means of adapting to changing environmental conditions and cellular requirements (Nussinov et al., 2013). In classic views of allostery (Monod et al., 1965; Koshland et al., 1966), effector binding at a distal site changes protein structure to affect function. For enzymes, these structural changes can affect substrate binding, catalytic efficiency and interactions with other macromolecules. In the "mechanical linkage" model, signals from allosteric effectors propagate through sequential structural changes from the distal site to other regions of the protein (Yu and Koshland, 2001). Amino acid residues that are key to these structural transitions comprise an amino acid interaction network (Süel et al., 2003; Amitai et al., 2004; Böde et al., 2007; Grewal and Roy, 2015; Dokholyan, 2016; O'Rourke et al., 2016). This well-ordered view of

progressive structural changes appears to stand in contrast to those systems in which allosteric ligands change protein function but do not substantially change protein structure (Popovych et al., 2006; Das et al., 2009; Tzeng and Kalodimos, 2009; Capdevila et al., 2017; Saavedra et al., 2018). In these systems, allosteric effectors may change structural dynamics or conformational sampling to affect interactions with other molecules. In this "dynamically driven allostery" (Cooper and Dryden, 1984; Reinhart et al., 1989; Petit et al., 2009; Motlagh et al., 2014; Kornev and Taylor, 2015; Nussinov and Tsai, 2015; Tzeng and Kalodimos, 2015; Guo and Zhou, 2016; Saavedra et al., 2018), key residues may still guide changes to protein structural dynamics (Rodgers et al., 2013; McLeish et al., 2015; Capdevila et al., 2017).

We have previously used the alpha subunit of tryptophan synthase as a model system for understanding amino acid interaction networks in proteins (Axe et al., 2014). Tryptophan synthase is composed of both alpha (αTS) and beta (βTS) subunits aligned in an αββα manner (i.e., a heterotetramer ~143 kDa in size) and is known for the ability to channel the αTS product indole directly into the active site of βTS through a 25 Å hydrophobic tunnel (Dunn, 2012). The αTS enzyme catalyzes the retro-aldol cleavage of the C3′-C3 bond of indole-3-glycerol phosphate (IGP) to form indole and glyceraldehyde-3-phosphate. The αTS enzyme has a $(\beta/\alpha)_8$ or TIM (triose phosphate isomerase) barrel structure with three additional α-helices (**Figure 1**). The α0 helix is located at the N-terminus of the protein, the α2′ helix (residues 62–74) is located between the β2 strand and the α2 helix, and the α8′ helix is located between the β8 strand and the α8 helix. Like other TIM barrel enzymes (Sterner and Höcker, 2005), the active site consists mostly of residues on the inner β-strands and the βα loops that connect β-strands to the following α-helices. The αβ loops that connect the α-helices to the β-strands tend to be shorter, and important for structural stability (Sterner and Höcker, 2005). Major structural changes in αTS are localized to the β2α2 and β6α6 loops. In the absence of βTS, the β2α2 loop extends through the α2' helix to include residues 52–77 (Nishio et al., 2005). The β6α6 loop encompasses residues 179–192 and is disordered in the absence of ligands (Kulik et al., 2002; Ngo et al., 2007; Barends et al., 2008; Lai et al., 2011). Upon binding IGP, αTS forms a closed conformation in which these loops make important hydrogen bonding interactions between Ala59, Asp60, and Gly61 on the β2α2 loop and Thr183 on the β6α6 loop. These events are likely important for positioning the catalytic residues Glu49 (on the β2 strand) and Asp60 (**Figure 1**).

We previously used NMR chemical shift covariance analysis (CHESCA; Selvaratnam et al., 2011; Boulton et al., 2018) to identify amino acid interaction networks in αTS, in the absence of βTS (Axe et al., 2014). Perturbation of these networks was shown to modulate αTS catalytic activity (Axe et al., 2014) and functional interactions with βTS (data not shown). Intriguingly, the amino acid interaction networks were substantially different between the apo *resting* state and the *working* state enzyme, which represents a catalytically-active state under a 4:1 dynamic chemical equilibrium between substrate- and products-bound enzyme (Axe and Boehr, 2013).

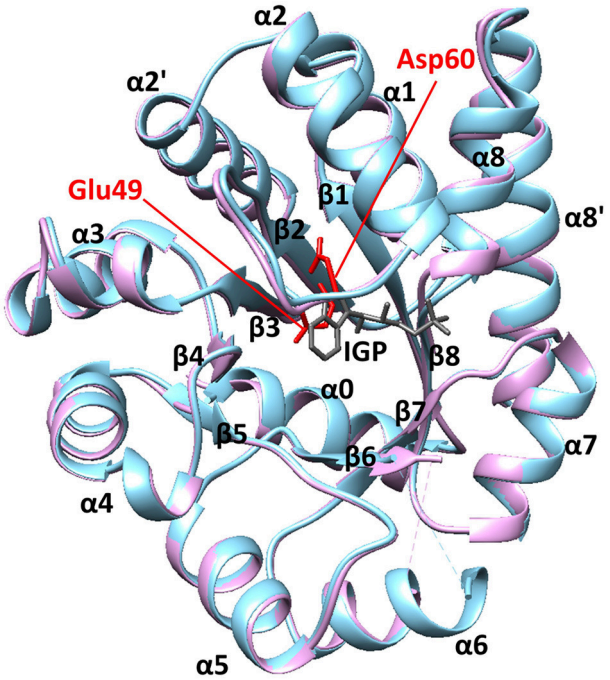

FIGURE 1 | The structure of αTS. These X-ray crystal structures are from *Salmonella typhimurium*, which has 85% sequence identity with *E.coli* αTS used in the NMR experiments. The blue and pink structures represent the ligand-free (PDB 1KFJ) and IGP-bound (PDB 2RHG) states, respectively. Binding of IGP substrate does not substantially change the ground-state αTS structure in the αTS-βTS tryptophan synthase complex.

The lack of structural differences between ligand-free and IGP-bound αTS suggested that changes in αTS conformational dynamics were likely the driving force behind differences in the NMR-derived networks. Indeed, our previous NMR studies indicated that the β2α2 and β6α6 loops were conformationally dynamic on multiple timescales (Axe and Boehr, 2013), but the millisecond timescale motions were suppressed in the *working* state (Axe and Boehr, 2013). In contrast, the picosecond-to-nanosecond timescale dynamics were rather ligand-independent (Axe and Boehr, 2013). Unfortunately, these previous studies were limited to Ala resonances, so could not provide information about the whole αTS enzyme.

To gain more insight into the relationships between structural dynamics and amino acid interaction networks in αTS, we characterized the millisecond timescale structural dynamics in the *resting*, *working*, indole-bound and G3P-bound states, using NMR ^{15}N R_2 relaxation dispersion experiments (Loria et al., 1999a,b). Interactions with ligands quenched some of the *resting* state motions, but induced motion in other areas of the enzyme. Many of the previously identified network residues displayed millisecond conformational exchange or were in close association with dynamic residues. This finding suggests that network changes can be relayed in part through changes in conformational motions.

RESULTS AND DISCUSSION

Conformational Exchange Events Across the Alpha Subunit of Tryptophan Synthase

To gain insight into conformational motions on the microsecond-to-millisecond timescale, we conducted ^{15}N R_2 relaxation dispersion experiments on αTS in various states, including the apo *resting* state, bound to the product indole (E:indole), bound to the product glyceraldehyde-3-phosphate (E:G3P), and under active turnover conditions in the *working* state (**Figure 2**). Active turnover conditions have been previously used to study conformational motions in the enzymes cyclophilin and adenylate kinase (Eisenmesser et al., 2002, 2005; Wolf-Watz et al., 2004).

We identified residues that were associated with more typical R_2 relaxation dispersion curves that could be fit assuming two-site exchange (purple spheres in **Figure 2**), and other residues whose resonances displayed exchange broadening and/or whose R_2 relaxation dispersion curves could not be reliably fit to kinetic or thermodynamic parameters (pink spheres in **Figure 2**). Some of the residues were also associated with higher than average R_2^0 values, which may be indicative of motions on a faster μs timescale. These experiments revealed that there were conformational exchange events throughout αTS under all conditions assessed, including in areas around the active site and in more distant regions, including on the outer α-helices. The pervasiveness of conformational exchange events around αTS would seem to be in contrast to previous X-ray crystal structure analyses of the *S. typhimurium* αTS-βTS, which indicated that ligand binding led to only local structural changes in αTS (Dierkers et al., 2009; Axe et al., 2014). A survey of β-factors in the X-ray crystal structures of isolated *E. coli* αTS (e.g., PDB 1XC4) also indicated that there was little dynamic disorder in the central β-strands, and the locations of conformational exchange identified by the ^{15}N R_2 relaxation dispersion experiments did not correspond to areas with higher β-factors. The conformational exchange events identified by the NMR experiments may be restricted in the crystal and/or reporting on a different timescale than the local atomic motions related to β-factors. The ^{15}N R_2 relaxation dispersion results on αTS are also in contrast to previous NMR relaxation studies on TIM itself, which indicated conformational exchange processes were generally localized around the β6α6 loop (Massi et al., 2006; Kempf et al., 2007).

Dynamic Networks in the Alpha Subunit of Tryptophan Synthase Are Switched on and Off by the Addition of Ligands

The ^{15}N R_2 relaxation dispersion experiments on the apo *resting* state enzyme indicated that αTS is intrinsically dynamic on the μs-ms timescale (**Figure 2**). To gain more insight into how ligand interactions may modulate protein motions, we identified conformational exchange events that were only present in the *resting* state (blue spheres in **Figure 2**) and those that were only present when the enzyme was bound with the products or in the *working* state (red spheres in **Figure 2**). As a caveat to the following analysis, we note that the inability to detect conformational exchange by the ^{15}N R_2 relaxation dispersion experiments does not rule out conformational motions, but if present, these motions are outside the kinetic and thermodynamic windows accessible by these experiments. With this in mind, the presence of indole led to additional conformational exchange events around the indole-binding region (e.g., Ala129, Asp130 on the β4α4 loop, Tyr173 on the α5β6 loop), or otherwise near the active site (e.g., Val20 on the β1 strand). Indole binding also induced conformational exchange to more distant residues. Some of these residues are close to one another and can form potential linkages to residues at the active site. For example, Asp46 in the α1β2 loop is nearby Val20, but also nearby Ile41 in the α1 helix and Lys263 in the α8' helix, which is on the same α-helix as Val257 and Phe258. We do not expect that these indole-induced conformational exchange events are due simply to indole binding/release from the enzyme as we expect the enzyme to be fully saturated with indole under these conditions, and some of the indole-induced changes are similar to the changes induced by the presence of G3P, which we would not expect if the conformational exchange events were simply reporting on binding/release of ligands. However, we note that indole is released first in the αTS kinetic mechanism (Weischet and Kirschner, 1976), so the indole-bound complex may have limited functional relevance.

The binding of G3P both induces and represses conformational exchange events compared to the *resting* state enzyme (**Figure 2**). For example, the dynamic residue cluster associated with the indole-binding site encompassed additional residues, including Ala116 in the α3 helix, Leu144 in the α4 helix, His146 and Val148 in the α4β5 loop, Ala149 in the β5 strand, and Arg171 in the α5β6 loop. These dynamic connections may help to explain why G3P binding leads to large chemical shift changes in some of these associated resonances despite these amino acid residues being more distant from the G3P-binding site (Axe and Boehr, 2013). The presence of G3P also led to the loss of conformational exchange events around the active site and outlying regions. For example, Ile232 near the phosphate-binding site and nearby residues (e.g., Gly17 in the α0β1 loop, Val220, and Ala223 in the α7 helix, and Ala231 in the β8 strand) did not show conformational exchange in the presence of G3P. Binding of G3P may act to stabilize this region and suppress conformational dynamics. Overall, there appears to be distinct regions in αTS in which conformational motions are essentially switched "on" or "off" by the presence of G3P.

The *working* state induced very similar changes to the conformational exchange events as G3P binding (**Figure 2**). Nonetheless, conformational exchange events in the *working* state did not simply reflect a combination of the conformational exchange events in the indole-bound and G3P-bound complexes. Specifically, some of the dynamic clusters discussed above for the product-bound complexes were repressed or modified in the *working* state. Residues near the indole ring (i.e., Leu100, Met101, Ser125) and a cluster of amino acid residues in the α0β1 loop (Gly17), β1 strand (Ala18, Val20), α1β2 loop (Asp46, Ala47), α7 helix (Ala223), and β8 strand (Ala231 and Ile232) did not show conformational exchange in the *working* state.

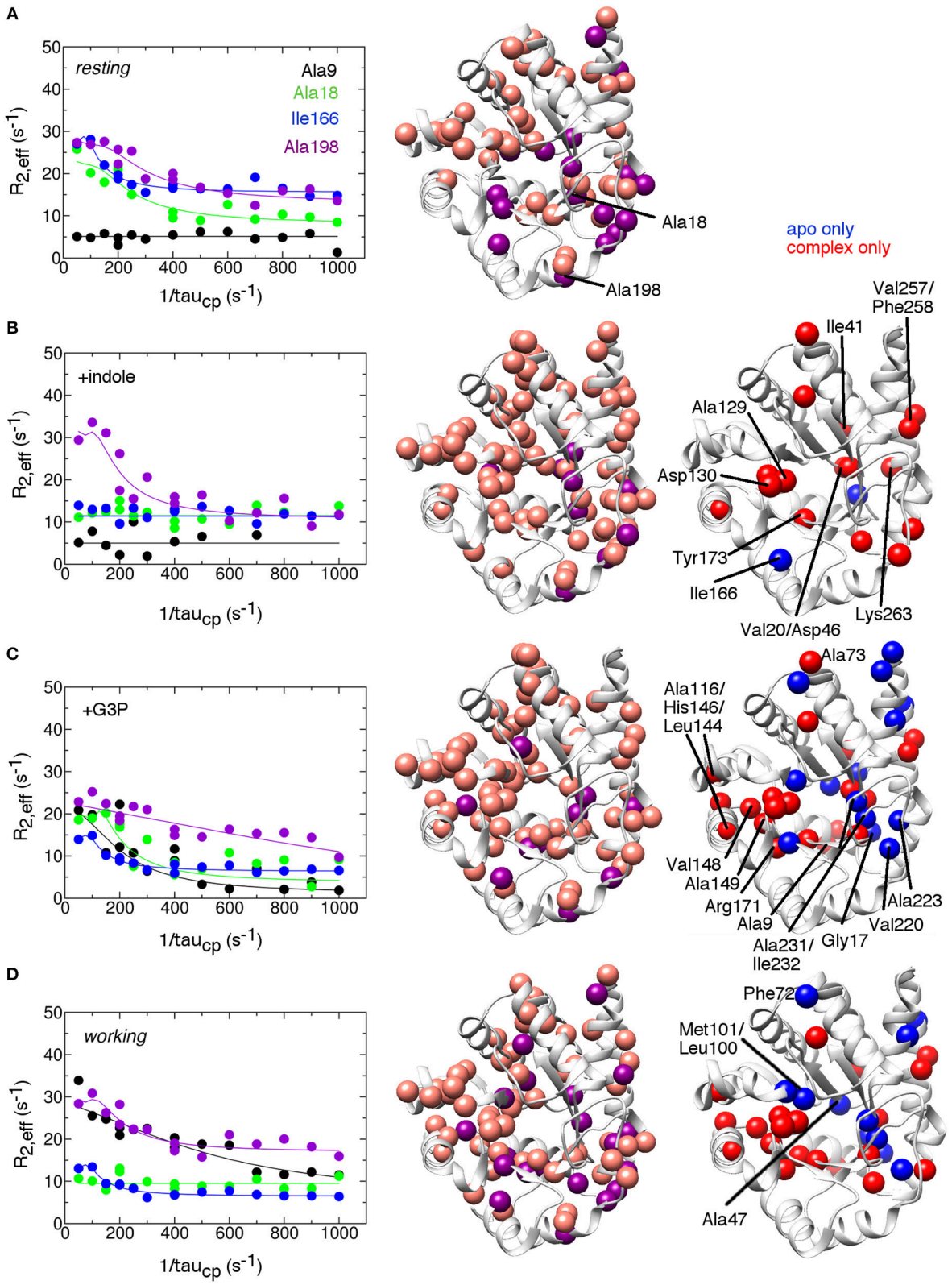

FIGURE 2 | Conformational exchange events in the *E.coli* αTS enzyme **(A)** in the apo *resting* state, **(B)** bound to product indole, **(C)** bound to the product glyceraldehyde-3-phosphate (G3P) and **(D)** in the *working* state under catalytic turnover. The *working* state represents a 4:1 ratio of enzyme bound with substrate indole-3-glycerol phosphate (IGP) to enzyme bound with products indole and G3P (Axe and Boehr, 2013; Axe et al., 2014). (left) example ^{15}N R_2 relaxation dispersion

(Continued)

FIGURE 2 | curves collected at a ^{1}H Larmor frequency of 850 MHz for the resonances belonging to Ala9 (black), Ala18 (green), Ile166 (blue), and Ala198 (purple). (middle) locations of conformational exchange according to the R_2 relaxation dispersion experiments plotted as spheres onto the αTS structure. Here, we used the *S.typhimurium* αTS structure bound to glyceraldehyde-3-phosphate (PDB 2CLK) as it contains resolved β2α2 and β6α6 loops. Purple spheres indicate that associated R_2 relaxation dispersion curves can be fit to two-site exchange, while pink spheres indicate exchange broadening, but the R_2 relaxation dispersion curves cannot be fit reliably to two-site exchange. (right) a comparison of the conformational exchange events in the *resting* apo state compared to when αTS is bound with ligands. Blue (red) spheres indicate conformational exchange events present in the apo (ligand-bound) state but not in the ligand-bound (apo) state. Most of the amino acid residues associated with a change in conformational dynamics make contact and/or near each other in three-dimensional space. The R_2 relaxation dispersion experiments were conducted at 283 K using a buffer consisting of 50 mM potassium phosphate, pH 7.8, 2 mM DTT, 0.2 mM Na_2EDTA, and 10% $^{2}H_2O$, and 0.5–1.0 mM protein with 10 mM indole and/or 20 mM G3P where appropriate.

Residues in the extended β2α2 (Phe72, Ala73) and β6α6 (Leu191) loops also did not show conformational exchange, suggesting that these loops become less conformationally dynamic during catalytic turnover. The suppression of conformational dynamics near the indole-binding pocket and at the active site loops may be important for binding ligands and maintaining an environment conducive to chemical catalysis. With that said, it is interesting that Glu49 and other residues in the β2 strand remain conformationally dynamic. X-ray crystal structures suggest that there is a reorientation of Glu49 when IGP binds (Rhee et al., 1998); conformational exchange events in this region may be reporting in part on this reorientation.

It is also worth noting that residues at or near the αTS/βTS interface region, including the α3 helix and the β4α4 and β5α5 loops, showed millisecond conformational motions in all or most complexes (**Figure 3**). These regions may be sampling conformations conducive to interactions with βTS, or may simply be more flexible without the structural constraints imposed by βTS binding.

Kinetic and Thermodynamic Assessment of the Conformational Exchange Events in the Alpha Subunit of Tryptophan Synthase

In favorable circumstances, R_2 relaxation dispersion experiments can also provide kinetics and thermodynamics information about the conformational exchange processes (Loria et al., 1999a,b). For two-site exchange between conformations A and B, R_2 relaxation dispersion experiments can yield the exchange rate constant k_{ex} that is the sum of the forward (k_{AB}) and reverse (k_{BA}) rate constants, the populations of the exchanging conformations (p_A, p_B), and the dynamic chemical shift difference between the exchanging conformations ($\Delta\omega = \delta\omega_A\text{-}\delta\omega_B$). Unfortunately, many of the ^{15}N R_2 relaxation dispersion curves would not fit according to a two-site exchange model and/or one or more data points were sufficiently off the fitted curve, likely owing to noise, to have confidence in the fitted parameters. Those residues that could fit reliably to a two-site exchange model had similar exchange kinetics and populations, so these residues were fit with global k_{ex} and p_A/p_B values (**Table 1**) and residue-specific Δω values. The *resting*, indole-bound and *working* states all had similar global k_{ex} values, whereas the G3P-bound state had a substantially lower global k_{ex} value. It should be noted that the rate constants reported here (e.g., $k_{A\rightarrow B}$ for the *working* state is 15 s^{-1} at 283 K) are substantially larger than the k_{cat} for αTS (k_{cat} ∼ 0.01 s^{-1} at 298 K). In other enzymes, such as dihydrofolate reductase (Boehr et al., 2006) and ribonuclease A (Beach et al., 2005), the dynamic chemical shift differences (i.e., Δω values) were used to indicate that these enzymes fluctuate into previously identified states (Boehr et al., 2009), however this was not the case for αTS (data not shown).

TABLE 1 | Kinetic and thermodynamics parameters for the millisecond motions in the alpha subunit of tryptophan synthase at 283 K.

State	k_{ex} (s^{-1})	p_A (%)	p_B (%)	k_{AB} (s^{-1})	k_{BA} (s^{-1})
Resting	286 ± 58	94.2	5.8	17	269
+indole	287 ± 25	90.0	10.0	29	254
+G3P	146 ± 21	93.0	7.0	10	136
Working	273 ± 19	94.4	5.6	15	258

Comparison of Chemical Shift-Based Amino Acid Interaction Networks and Conformational Exchange Events in the Alpha Subunit of Tryptophan Synthase

We had previously identified amino acid interaction networks in αTS using the CHESCA (chemical shift covariance analysis) method (Axe et al., 2014). In short, we identified clusters of amino acid residues that responded in a similar fashion to a set of Ala-to-Gly perturbations, those being A59G, A67G, A158G, A180G, and A185G where Ala59 and Ala67 are on the extended β2α2 loop, Ala158 is on the β5α5 loop, and Ala180, and Ala185 are on the β6α6 loop. The β2α2, β5α5, and β6α6 loops are all known to contribute to αTS-βTS communication and indole channeling (Lim et al., 1991a,b; Hiraga and Yutani, 1997; Dunn, 2012). Intriguingly, the composition of one of these clusters substantially changed between the *resting* and *working* states (Axe et al., 2014). We proposed that this cluster was especially important for αTS function, considering that the catalytic residue Glu49 becomes part of this cluster only in the *working* state. Molecular dynamics (MD) simulations also indicated that Glu49 has coordinated motional trajectories with this *working* state cluster (Ai et al., 2010; Fatmi and Chang, 2010). With this in mind, we focused only on the CHESCA cluster that changes between the *resting* and *working* states of αTS.

Consistent with the MD simulations, only a few CHESCA cluster residues showed conformational exchange according to the ^{15}N R_2 relaxation dispersion experiments (**Figure 3**, green spheres), whereas the majority of the CHESCA cluster residues showed conformational exchange in the *working* state. In fact, the CHESCA cluster residues that did not show

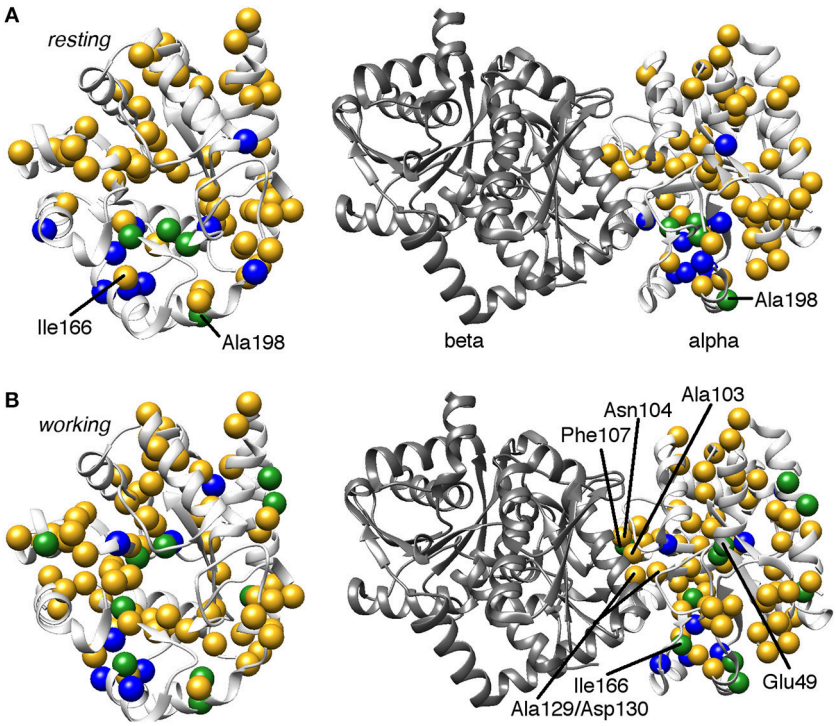

FIGURE 3 | Comparison of conformational exchange events identified by ^{15}N R_2 relaxation dispersion experiments and a residue cluster identified by chemical shift covariance analysis (CHESCA) for the **(A)** apo *resting* and **(B)** *working* states of *E. coli* αTS. The *working* state represents active catalytic turnover conditions in which there is a 4:1 ratio of enzyme bound with substrate indole-3-glycerol phosphate (IGP) to enzyme bound with products indole and G3P (Axe and Boehr, 2013; Axe et al., 2014). Yellow spheres indicate μs-ms timescale conformational exchange events identified by ^{15}N R_2 relaxation dispersion experiments (i.e., pink and purple spheres in **Figure 2**), blue spheres indicate residues belonging to the previously identified CHESCA cluster, and green spheres indicate CHESCA cluster residues that show conformational exchange. The same information is presented on (left) the αTS structure and (right) the full TS complex (PDB 2CLK). It should be noted that all NMR data were collected in the absence of βTS. Nonetheless, there are conformational exchange events and CHESCA cluster residues near the βTS-binding interface, which may be important in the context of the full TS complex. There are more CHESCA cluster residues showing conformational exchange in the *working* state compared to the *resting* state.

conformational exchange (**Figure 3**, blue spheres) in the *working* state were immediately adjacent to other residues that were conformationally dynamic on the μs-ms timescale (**Figure 3**, yellow spheres). Especially in the *working* state, paths of interactions can be traced connecting the CHESCA cluster residues through residues undergoing conformational exchange (**Figure 4**).

CONCLUSION

We had previously identified amino acid interaction networks in the isolated αTS subunit, in the absence of the βTS subunit. These networks were different between the *resting* and *working* states of the enzyme. Unfortunately, the changes in the networks could not be explained by structural considerations alone considering the structural similarity between ligand-free and ligand-bound αTS (at least in the context of the αTS-βTS complex) (Axe et al., 2014). However, MD simulations suggested that network residues had coupled motions (Axe et al., 2014), prompting the study of protein structural dynamics by NMR. Indeed, the ^{15}N R_2 relaxation dispersion studies indicated that the *resting* and *working* states of the enzyme had some different dynamic features on the μs-ms timescale. Ligand binding appeared to enable or suppress the millisecond motions of paths or clusters of residues, or in the very least, changed which residues have detectable conformational exchange within the limits of the ^{15}N R_2 relaxation dispersion experiments. Previously identified network residues were conformationally dynamic, or interacted with dynamic residues, suggesting that information through these networks may be conducted by changes in conformational motions in the absence of detectable structural changes. These results suggest networks in proteins (at least those identified by CHESCA) do not simply reflect structural interactions in the lowest energy, ground-state conformation, but rather these networks also reflect motional coupling and/or interactions as proteins fluctuate into higher energy protein conformations. This network view is more complex than the "mechanical linkage" model (Yu and Koshland, 2001) in which allosteric signals propagate through sequential structural changes in a "domino-like" fashion, and is more compatible with dynamically driven allostery (Cooper and Dryden, 1984; Reinhart et al., 1989; Petit et al., 2009; Motlagh et al., 2014;

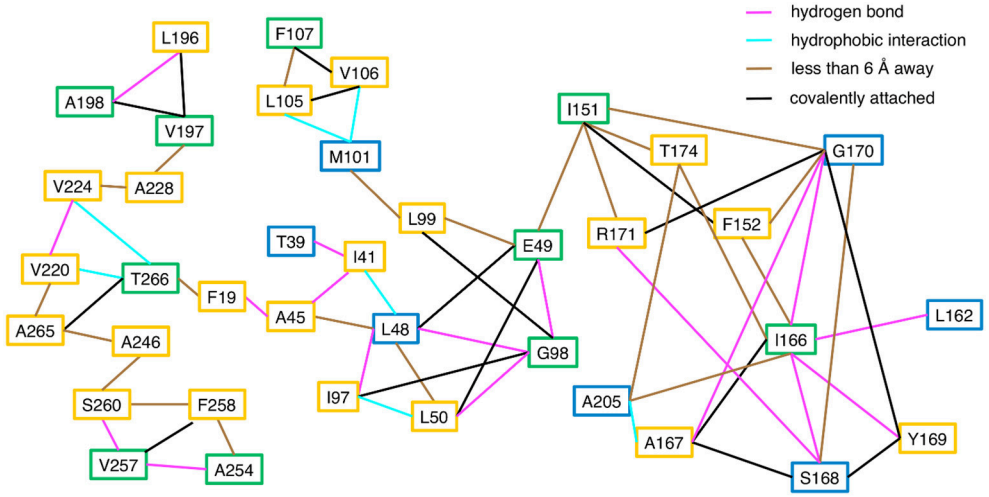

FIGURE 4 | Connections between CHESCA network and exchanging residues in the *working* state enzyme. Residues that show millisecond conformational exchange according to ^{15}N R_2 relaxation dispersion studies are boxed in yellow, residues that were previously identified to be CHESCA network residues (Axe et al., 2014) are boxed in blue, and residues that are CHESCA network residues and show conformational exchange are boxed in green. Lines indicate the type of interaction between the residues, including hydrogen bond (pink line), a hydrophobic interaction (cyan line), covalently attached (black line), or within at least 6 Å distance where side chain motion may lead to contact. CHESCA network residues either undergo conformational exchange or interact with residues that undergo conformational exchange.

Kornev and Taylor, 2015; Nussinov and Tsai, 2015; Tzeng and Kalodimos, 2015; Guo and Zhou, 2016; Saavedra et al., 2018).

The dynamic networks identified in isolated αTS may also be important in the context of the full αTS-βTS complex. Some motions were induced near the αTS/βTS binding interface upon binding ligands (e.g., Ala129, Asp130), whereas other residues were structurally dynamic also in the apo state (e.g., Asn104). Amino acid substitutions at these positions are known to affect αTS-βTS function and stability (Lim et al., 1991a,b; Yang et al., 2007). Computer simulations also suggested that interactions between αTS and βTS in the full complex are dependent on ligand binding (Fatmi and Chang, 2010), which might be reflected by a change in conformational dynamics. The T183V substitution, known to affect substrate channeling, also affects the CHESCA networks (Axe et al., 2015), and amino acid substitutions at network positions affect αTS function (Axe et al., 2014). Analysis of network substitutions may also reveal how the αTS networks are important for function in the full αTS-βTS complex. However, it should be kept in mind that binding of βTS may change or restrict these motions, which would likely have further dynamic effects throughout αTS. A comparison of αTS structural dynamics in the absence and presence of βTS may reveal those motions most important for communication within the full enzyme complex. Unfortunately, we were unable to collect ^{15}N R_2 relaxation dispersion data for the full αTS-βTS complex, likely owing to its large size (i.e. 143 kDa). Nonetheless, preliminary studies suggest that ^{13}C-methyl experiments may be possible for the full enzyme complex similar to studies in other large protein complexes (Velyvis et al., 2009a,b). These studies may reveal dynamic networks in αTS-βTS similar to the dynamic networks revealed in another substrate-channeling enzyme imidazole glycerol phosphate synthase (ImGPS), involved in histidine biosynthesis. In ImGPS, allosteric pathways were initially identified based on community analysis of MD simulations (Rivalta et al., 2012). Amino acid substitutions at network positions in HisH resulted in the suppression of millisecond timescale dynamics and decreased enhancement of HisF catalytic activity (Lisi et al., 2017). These studies also suggest that network changes can be conducted through changes in conformational exchange dynamics in the absence of notable ground-state structural differences.

MATERIALS AND METHODS

Overexpression and Purification of αTS Samples

All samples were overexpressed using *Escherichia coli* BL21(DE3*) cells grown in either Luria-Bertani media (EMD Millipore, Billerica, MA, USA) or M9 minimal media for NMR experiments. Samples for backbone relaxation dispersion were grown in $^{2}H_2O$-based media with ^{15}N-labeled ammonium chloride (Cambridge Isotopes, Tewksbury, MA, USA).

All samples were purified using an anion-exchange column Q-sepharose (GE Healthcare, Pittsburgh, PA, USA) with buffers A (25 mM HEPES, pH 7.5, 1 mM Na_2EDTA) and B (buffer A with 1 M NaCl) using a 0–50% gradient of buffer B. Samples were concentrated with a Corning Spin-X UF centrifugal concentrator (Sigma Aldrich, St. Louis, MO, USA) to a volume of ∼1 mL then purified on a S100 gel filtration column (GE Healthcare) in buffer A with 200 mM NaCl.

NMR Sample Preparation and Experiments

Following purification, a ZEBA desalting column (Thermo Fisher) was used to exchange all ^{15}N-labeled samples into NMR buffer (50 mM potassium phosphate, pH 7.8, 2 mM DTT, 0.2 mM Na_2EDTA, and 10% ^2H_2O). The samples contained 0.5–1.0 mM protein with 10 mM indole (Thermo Fisher), 20 mM G3P (Sigma Aldrich), and/or 3 mM IGP where appropriate. All experiments were collected on Brüker (Billerica, MA, USA) Avance III spectrometers.

^{15}N R_2 Relaxation Dispersion Experiments

^{15}N R_2 relaxation dispersion experiments were collected at 283K on 600 and 850 MHz spectrometers. R_2 relaxation rates were measured using relaxation-compensated CPMG (Carr-Purcell-Meiboom-Gill) pulse sequences in a constant time manner (Loria et al., 1999a,b). The total CPMG period was 40 ms. Where appropriate, data was fit to the following equations for exchange between two sites:

$$R_2\left(\frac{1}{\tau_{CP}}\right) = R_2^0 + \frac{1}{2}\left[k_{ex} - \frac{1}{\tau_{CP}} cosh^{-1}\left(D_+ cosh\left(\eta_+\right) - D_- cos\left(\eta_-\right)\right)\right]$$

Where,

$$D_\pm = \frac{1}{2}\left[\pm 1 + \frac{\Psi + 2\Delta\omega^2}{\left(\Psi^2 + \zeta^2\right)^{1/2}}\right]^{1/2} \text{ and } \eta_\pm = \frac{\tau_{CP}}{2}\left[\pm\Psi + \left(\Psi^2 + \zeta^2\right)^{1/2}\right]^{1/2}$$

using the computer program GLOVE (Sugase et al., 2013). In these equations, $\Psi = kex^2 - \Delta\omega^2$, $\zeta = -2\ \Delta\omega k_{ex}(p_A - p_B)$, τ_{CP} is the time between 180° pulses in the CPMG segment, R_2^0 is the R_2 relaxation rate in the absence of conformational exchange, p_A and p_B are the populations of states A and B, k_{ex} is the rate of exchange between states A and B, and $\Delta\omega$ is the difference in the chemical shift between states A and B.

DATA AVAILABILITY

The raw data supporting the conclusions of this manuscript will be made available by the authors, without undue reservation, to any qualified researcher.

AUTHOR CONTRIBUTIONS

KO, JA, and DB contributed to the conception and design of the study. KO, JA, and RD generated protein samples. KO and JA collected ^{15}N R_2 relaxation dispersion data. DS supplied technical advice with the implementation of the ^{15}N R_2 relaxation dispersion experiments. KO and DB generated figures. KO and DB wrote the manuscript. All authors contributed to manuscript revision, read and approved the submitted version.

FUNDING

This work was supported by National Science Foundation (NSF) grant MCB-1615032.

ACKNOWLEDGMENTS

We thank Scott Gorman and Alyson Boehr for comments on the manuscript and discussions about enzyme structural dynamics and allostery.

REFERENCES

Ai, R., Qaiser Fatmi, M., and Chang, C. E. (2010). T-Analyst: a program for efficient analysis of protein conformational changes by torsion angles. *J. Comput. Aid. Mol. Des.* 24, 819–827. doi: 10.1007/s10822-010-9376-y

Amitai, G., Shemesh, A., Sitbon, E., Shklar, M., Netanely, D., Venger, I., et al. (2004). Network analysis of protein structures identifies functional residues. *J. Mol. Biol.* 344, 1135–1146. doi: 10.1016/j.jmb.2004.10.055

Axe, J. M., and Boehr, D. D. (2013). Long-range interactions in the alpha subunit of tryptophan synthase help to coordinate ligand binding, catalysis, and substrate channeling. *J. Mol. Biol.* 425, 1527–1545. doi: 10.1016/j.jmb.2013.01.030

Axe, J. M., O'Rourke, K. F., Kerstetter, N. E., Yezdimer, E. M., Chan, Y. M., Chasin, A., et al. (2015). Severing of a hydrogen bond disrupts amino acid networks in the catalytically active state of the alpha subunit of tryptophan synthase. *Protein Sci.* 24, 484–494. doi: 10.1002/pro.2598

Axe, J. M., Yezdimer, E. M., O'Rourke, K. F., Kerstetter, N. E., You, W., Chang, C. E., et al. (2014). Amino acid networks in a (beta/alpha)(8) barrel enzyme change during catalytic turnover. *J. Am. Chem. Soc.* 136, 6818–6821. doi: 10.1021/ja501602t

Barends, T. R., Domratcheva, T., Kulik, V., Blumenstein, L., Niks, D., Dunn, M. F., et al. (2008). Structure and mechanistic implications of a tryptophan synthase quinonoid intermediate. *ChemBioChem* 9, 1024–1028. doi: 10.1002/cbic.200700703

Beach, H., Cole, R., Gill, M. L., and Loria, J. P. (2005). Conservation of mus-ms enzyme motions in the apo- and substrate-mimicked state. *J. Am. Chem. Soc.* 127, 9167–9176. doi: 10.1021/ja0514949

Böde, C., Kovács, I. A., Szalay, M. S., Palotai, R., Korcsmáros, T., and Csermely, P. (2007). Network analysis of protein dynamics. *FEBS Lett.* 581, 2776–2782. doi: 10.1016/j.febslet.2007.05.021

Boehr, D. D., McElheny, D., Dyson, H. J., and Wright, P. E. (2006). The dynamic energy landscape of dihydrofolate reductase catalysis. *Science* 313, 1638–1642. doi: 10.1126/science.1130258

Boehr, D. D., Nussinov, R., and Wright, P. E. (2009). The role of dynamic conformational ensembles in biomolecular recognition. *Nat. Chem. Biol.* 5, 789–796. doi: 10.1038/nchembio.232

Boulton, S., Selvaratnam, R., Ahmed, R., and Melacini, G. (2018). Implementation of the NMR CHEmical Shift Covariance Analysis (CHESCA): a chemical biologist's approach to allostery. *Methods Mol. Biol.* 1688, 391–405. doi: 10.1007/978-1-4939-7386-6_18

Capdevila, D. A., Braymer, J. J., Edmonds, K. A., Wu, H., and Giedroc, D. P. (2017). Entropy redistribution controls allostery in a metalloregulatory protein. *Proc. Natl. Acad. Sci. U.S.A.* 114, 4424–4429. doi: 10.1073/pnas.1620665114

Cooper, A., and Dryden, D. T. (1984). Allostery without conformational change. A plausible model. *Eur. Biophys. J.* 11, 103–109. doi: 10.1007/BF00276625

Das, R., Chowdhury, S., Mazhab-Jafari, M. T., Sildas, S., Selvaratnam, R., and Melacini, G. (2009). Dynamically driven ligand selectivity in

cyclic nucleotide binding domains. *J. Biol. Chem.* 284, 23682–23696. doi: 10.1074/jbc.M109.011700

Dierkers, A. T., Niks, D., Schlichting, I., and Dunn, M. F. (2009). Tryptophan synthase: structure and function of the monovalent cation site. *Biochemistry* 48, 10997–11010. doi: 10.1021/bi9008374

Dokholyan, N. V. (2016). Controlling allosteric networks in proteins. *Chem. Rev.* 116, 6463–6487. doi: 10.1021/acs.chemrev.5b00544

Dunn, M. F. (2012). Allosteric regulation of substrate channeling and catalysis in the tryptophan synthase bienzyme complex. *Arch. Biochem. Biophys.* 519, 154–166. doi: 10.1016/j.abb.2012.01.016

Eisenmesser, E. Z., Bosco, D. A., Akke, M., and Kern, D. (2002). Enzyme dynamics during catalysis. *Science* 295, 1520–1523. doi: 10.1126/science.1066176

Eisenmesser, E. Z., Millet, O., Labeikovsky, W., Korzhnev, D. M., Wolf-Watz, M., Bosco, D. A., et al. (2005). Intrinsic dynamics of an enzyme underlies catalysis. *Nature* 438, 117–121. doi: 10.1038/nature04105

Fatmi, M. Q., and Chang, C. E. (2010). The role of oligomerization and cooperative regulation in protein function: the case of tryptophan synthase. *PLoS Comput. Biol.* 6:e1000994. doi: 10.1371/journal.pcbi.1000994

Grewal, R. K., and Roy, S. (2015). Modeling proteins as residue interaction networks. *Protein Pept. Lett.* 22, 923–933. doi: 10.2174/0929866522666150728115552

Guo, J., and Zhou, H. X. (2016). Protein allostery and conformational dynamics. *Chem. Rev.* 116, 6503–6515. doi: 10.1021/acs.chemrev.5b00590

Hiraga, K., and Yutani, K. (1997). Roles of hydrogen bonding residues in the interaction between the alpha and beta subunits in the tryptophan synthase complex. Asn-104 of the alpha subunit is especially important. *J. Biol. Chem.* 272, 4935–4940. doi: 10.1074/jbc.272.8.4935

Kempf, J. G., Jung, J. Y., Ragain, C., Sampson, N. S., and Loria, J. P. (2007). Dynamic requirements for a functional protein hinge. *J. Mol. Biol.* 368, 131–149. doi: 10.1016/j.jmb.2007.01.074

Kornev, A. P., and Taylor, S. S. (2015). Dynamics-driven allostery in protein kinases. *Trends Biochem. Sci.* 40, 628–647. doi: 10.1016/j.tibs.2015.09.002

Koshland, D. E. Jr., Némethy, G., and Filmer, D. (1966). Comparison of experimental binding data and theoretical models in proteins containing subunits. *Biochemistry* 5, 365–385. doi: 10.1021/bi00865a047

Kulik, V., Weyand, M., Seidel, R., Niks, D., Arac, D., Dunn, M. F., et al. (2002). On the role of alphaThr183 in the allosteric regulation and catalytic mechanism of tryptophan synthase. *J. Mol. Biol.* 324, 677–690. doi: 10.1016/S0022-2836(02)01109-9

Lai, J., Niks, D., Wang, Y., Domratcheva, T., Barends, T. R., Schwarz, F., et al. (2011). X-ray and NMR crystallography in an enzyme active site: the indoline quinonoid intermediate in tryptophan synthase. *J. Am. Chem. Soc.* 133, 4–7. doi: 10.1021/ja106555c

Lim, W. K., Sarkar, S. K., and Hardman, J. K. (1991a). Enzymatic properties of mutant *Escherichia coli* tryptophan synthase alpha-subunits. *J. Biol. Chem.* 266, 20205–20212.

Lim, W. K., Shin, H. J., Milton, D. L., and Hardman, J. K. (1991b). Relative activities and stabilities of mutant *Escherichia coli* tryptophan synthase alpha subunits. *J. Bacteriol.* 173, 1886–1893.

Lisi, G. P., East, K. W., Batista, V. S., and Loria, J. P. (2017). Altering the allosteric pathway in IGPS suppresses millisecond motions and catalytic activity. *Proc. Natl. Acad. Sci. U.S.A.* 114, E3414–E3423. doi: 10.1073/pnas.1700448114

Loria, J. P., Rance, M., and Palmer, A. G. (1999a). A relaxation-compensated Carr-Purcell-Meiboom-Gill sequence for characterizing chemical exchange by NMR spectroscopy. *J. Am. Chem. Soc.* 121, 2331–2332.

Loria, J. P., Rance, M., and Palmer, A. G. III. (1999b). A TROSY CPMG sequence for characterizing chemical exchange in large proteins. *J. Biomol. NMR* 15, 151–155.

Massi, F., Wang, C., and Palmer, A. G. III. (2006). Solution NMR and computer simulation studies of active site loop motion in triosephosphate isomerase. *Biochemistry* 45, 10787–10794. doi: 10.1021/bi060764c

McLeish, T. C., Cann, M. J., and Rodgers, T. L. (2015). Dynamic transmission of protein allostery without structural change: spatial pathways or global modes? *Biophys. J.* 109, 1240–1250. doi: 10.1016/j.bpj.2015.08.009

Monod, J., Wyman, J., and Changeux, J. P. (1965). On the nature of allosteric transitions: a plausible model. *J. Mol. Biol.* 12, 88–118. doi: 10.1016/S0022-2836(65)80285-6

Motlagh, H. N., Wrabl, J. O., Li, J., and Hilser, V. J. (2014). The ensemble nature of allostery. *Nature* 508, 331–339. doi: 10.1038/nature13001

Ngo, H., Kimmich, N., Harris, R., Niks, D., Blumenstein, L., Kulik, V., et al. (2007). Allosteric regulation of substrate channeling in tryptophan synthase: modulation of the L-serine reaction in stage I of the beta-reaction by alpha-site ligands. *Biochemistry* 46, 7740–7753. doi: 10.1021/bi7003872

Nishio, K., Morimoto, Y., Ishizuka, M., Ogasahara, K., Tsukihara, T., and Yutani, K. (2005). Conformational changes in the alpha-subunit coupled to binding of the beta 2-subunit of tryptophan synthase from *Escherichia coli*: crystal structure of the tryptophan synthase alpha-subunit alone. *Biochemistry* 44, 1184–1192. doi: 10.1021/bi047927m

Nussinov, R., and Tsai, C. J. (2015). Allostery without a conformational change? Revisiting the paradigm. *Curr. Opin. Struct. Biol.* 30, 17–24. doi: 10.1016/j.sbi.2014.11.005

Nussinov, R., Tsai, C. J., and Ma, B. (2013). The underappreciated role of allostery in the cellular network. *Annu. Rev. Biophys.* 42, 169–189. doi: 10.1146/annurev-biophys-083012-130257

O'Rourke, K. F., Gorman, S. D., and Boehr, D. D. (2016). Biophysical and computational methods to analyze amino acid interaction networks in proteins. *Comput. Struct. Biotechnol. J.* 14, 245–251. doi: 10.1016/j.csbj.2016.06.002

Petit, C. M., Zhang, J., Sapienza, P. J., Fuentes, E. J., and Lee, A. L. (2009). Hidden dynamic allostery in a PDZ domain. *Proc. Natl. Acad. Sci. U.S.A.* 106, 18249–18254. doi: 10.1073/pnas.0904492106

Popovych, N., Sun, S., Ebright, R. H., and Kalodimos, C. G. (2006). Dynamically driven protein allostery. *Nat. Struct. Mol. Biol.* 13, 831–838. doi: 10.1038/nsmb1132

Reinhart, G. D., Hartleip, S. B., and Symcox, M. M. (1989). Role of coupling entropy in establishing the nature and magnitude of allosteric response. *Proc. Natl. Acad. Sci. U.S.A.* 86, 4032–4036. doi: 10.1073/pnas.86.11.4032

Rhee, S., Miles, E. W., and Davies, D. R. (1998). Cryo-crystallography of a true substrate, indole-3-glycerol phosphate, bound to a mutant (alphaD60N) tryptophan synthase alpha2beta2 complex reveals the correct orientation of active site alphaGlu49. *J. Biol. Chem.* 273, 8553–8555. doi: 10.1074/jbc.273.15.8553

Rivalta, I., Sultan, M. M., Lee, N. S., Manley, G. A., Loria, J. P., and Batista, V. S. (2012). Allosteric pathways in imidazole glycerol phosphate synthase. *Proc. Natl. Acad. Sci. U.S.A.* 109, E1428–1436. doi: 10.1073/pnas.1120536109

Rodgers, T. L., Townsend, P. D., Burnell, D., Jones, M. L., Richards, S. A., McLeish, T. C., et al. (2013). Modulation of global low-frequency motions underlies allosteric regulation: demonstration in CRP/FNR family transcription factors. *PLoS Biol.* 11:e1001651. doi: 10.1371/journal.pbio.1001651

Saavedra, H. G., Wrabl, J. O., Anderson, J. A., Li, J., and Hilser, V. J. (2018). Dynamic allostery can drive cold adaptation in enzymes. *Nature* 558, 324–328. doi: 10.1038/s41586-018-0183-2

Selvaratnam, R., Chowdhury, S., VanSchouwen, B., and Melacini, G. (2011). Mapping allostery through the covariance analysis of NMR chemical shifts. *Proc. Natl. Acad. Sci. U.S.A.* 108, 6133–6138. doi: 10.1073/pnas.1017311108

Sterner, R., and Höcker, B. (2005). Catalytic versatility, stability, and evolution of the (betaalpha)8-barrel enzyme fold. *Chem. Rev.* 105, 4038–4055. doi: 10.1021/cr030191z

Süel, G. M., Lockless, S. W., Wall, M. A., and Ranganathan, R. (2003). Evolutionarily conserved networks of residues mediate allosteric communication in proteins. *Nat. Struct. Biol.* 10, 59–69. doi: 10.1038/nsb881

Sugase, K., Konuma, T., Lansing, J. C., and Wright, P. E. (2013). Fast and accurate fitting of relaxation dispersion data using the flexible software package GLOVE. *J. Biomol. NMR* 56, 275–283. doi: 10.1007/s10858-013-9747-5

Tzeng, S. R., and Kalodimos, C. G. (2009). Dynamic activation of an allosteric regulatory protein. *Nature* 462, 368–372. doi: 10.1038/nature08560

Tzeng, S. R., and Kalodimos, C. G. (2015). The role of slow and fast protein motions in allosteric interactions. *Biophys. Rev.* 7, 251–255. doi: 10.1007/s12551-015-0172-8

Velyvis, A., Schachman, H. K., and Kay, L. E. (2009a). Application of methyl-TROSY NMR to test allosteric models describing effects of nucleotide binding to aspartate transcarbamoylase. *J. Mol. Biol.* 387, 540–547. doi: 10.1016/j.jmb.2009.01.066

Velyvis, A., Schachman, H. K., and Kay, L. E. (2009b). Assignment of Ile, Leu, and Val methyl correlations in supra-molecular systems: an application

to aspartate transcarbamoylase. *J. Am. Chem. Soc.* 131, 16534–16543. doi: 10.1021/ja906978r

Weischet, W. O., and Kirschner, K. (1976). The mechanism of the synthesis of indoleglycerol phosphate catalyzed by tryptophan synthase from *Escherichia coli*. Steady-state kinetic studies. *Eur. J. Biochem.* 65, 365–373. doi: 10.1111/j.1432-1033.1976.tb10350.x

Wolf-Watz, M., Thai, V., Henzler-Wildman, K., Hadjipavlou, G., Eisenmesser, E. Z., and Kern, D. (2004). Linkage between dynamics and catalysis in a thermophilic-mesophilic enzyme pair. *Nat. Struct. Mol. Biol.* 11, 945–949. doi: 10.1038/nsmb821

Yang, X., Vadrevu, R., Wu, Y., and Matthews, C. R. (2007). Long-range side-chain-main-chain interactions play crucial roles in stabilizing the (betaalpha)8 barrel motif of the alpha subunit of tryptophan synthase. *Protein Sci.* 16, 1398–1409. doi: 10.1110/ps.062704507

Yu, E. W., and Koshland, D. E. Jr. (2001). Propagating conformational changes over long (and short) distances in proteins. *Proc. Natl. Acad. Sci. U.S.A.* 98, 9517–9520. doi: 10.1073/pnas.161239298

Conflict of Interest Statement: The authors declare that the research was conducted in the absence of any commercial or financial relationships that could be construed as a potential conflict of interest.